Available online at www.sciencedirect.com
SCIENCE DIRECT®
Thermochimica Acta 423 (2004) 137–141
thermochimica acta
www.elsevier.com/locate/tca

Thermal decomposition and molecular structure of 5-aminotetrazolium nitrate

Guixia Ma [a,*], Tonglai Zhang [a], Jianguo Zhang [a], Kaibei Yu [b]

[a] *Department of Mechano-electronic Engineering, State Key Laboratory of Prevention and Control of Explosion, Beijing Institute of Technology, Beijing 100081, PR China*
[b] *Chengdu Center of Analysis and Measurement, Chinese Academy of Sciences, Chengdu 610041, PR China*

Received 11 February 2004; received in revised form 6 May 2004; accepted 6 May 2004
Available online 24 June 2004

Abstract

The thermal decomposition of 5-aminotetrazolium nitrate (5-ATZN) was studied at a heating rate of 10 °C/min from 50 to 600 °C/min by DSC and TG techniques. Two intense exothermic processes are observed and the solid decomposition residues were thermally stable cyclic azines. Crystals of 5-ATZN were obtained from the aqueous solution by slow evaporation at room temperature. They crystallize in the monoclinic space group $P2_1/c$ with crystal parameters: $a = 1.0606(2)$ nm, $b = 0.35065(4)$ nm, $c = 1.4641(2)$ nm, $\beta = 90.63(1)^\circ$, $V = 0.5444(1)$ nm^3, $Z = 4$, $D_c = 1.807$ g/cm^3, μ(MoKα) $= 0.168$ mm^{-1}, $F(000) = 304$. The structure consists of NO_3^- anions and $[5\text{-ATZH}]^+$ cations, of which the 4-N was protonized. Electrostatic interaction and intermolecular hydrogen bonds assemble the ions into 2D layered structures.

Keywords: 5-Aminotetrazolium nitrate; Thermal decomposition mechanism; Molecular structure

1. Introduction

5-Aminotetrazolium nitrate (5-ATZN) is an unstable oxygen-rich compound used for inflating air bags and actuating seatbelt pre-tensioners in passenger-restraint devices. Gas-generating composite propellants based on 5-ATZN as the oxidant were disclosed in 1969 by Moy et al. [1]. These gas generators were found to have better burning rates, increased temperature stability, higher non-corrosive gas volumes, a minimum of solid particulates and lower flame temperatures over those of earlier ammonium nitrate gas generators [1–4]. All these properties are highly desirable for gas-generating propellants.

As indicated by Stoner and Brill [5], combustion is likely to be dominated by condensed-phase decomposition processes, so it is necessary to explore the thermal decomposition mechanism of 5-ATZN. Previous thermal decomposition studies on 5-ATZ and its derivatives revealed the formation of thermally stable cyclic azine residues, which are supposed to suppress the burning rates, to enhance the combustion stability, and to decrease the temperature sensitivity of propellants containing 5-ATZ [6,7]. An investigation conducted on the hydrohalide salts of 5-ATZ by a T-Jump/FT-IR method indicated that the proton donor ability of the acid determines the thermal decomposition route and hence the solid residues [8]. One pathway is the dissociation of the salt to form HX (X = Cl, Br, I) and 5-ATZ, and another involves the decomposition of the $[5\text{-ATZH}]^+$ ion directly. In this paper, the thermal decomposition of 5-ATZN has been studied at a heating rate of 10 °C/min and a pressure of 0.2 MPa by DSC and TG techniques. The molecular structure of 5-ATZN is also reported here.

2. Experimental

2.1. Synthesis of 5-ATZN

5-ATZ·H_2O was prepared according to the method given by Zhang et al. [9]. Nitric acid aqueous solution (65 mass%) of analytical grade was purchased from Beijing Chemical Co. and diluted to 20 mass% before use.

* Corresponding author. Tel.: +86-10-68913818; fax: +86-10-68911202.
E-mail address: ztlbit@public.bta.net.cn (G. Ma).

0040-6031/$ – see front matter © 2004 Elsevier B.V. All rights reserved.
doi:10.1016/j.tca.2004.05.004

5-ATZN was synthesized as follows: 20 g (0.194 mol) of 5-ATZ·H_2O, 71 mL (0.252 mol) of nitric acid solution and 50 mL of water were stirred for about 1 h in a water bath at 70 °C. The resulting colorless solution was cooled to room temperature while stirring. On slow evaporation at room temperature, colorless crystals of 5-ATZN were obtained after about 4 weeks with an approximate yield of 65% based on the initial 5-ATZ·H_2O inputs. Elemental analysis for 5-ATZN (molar mass 148.1 g/mol) (%): Calculated: C 8.11; N 56.75; H 2.72; Found: C 8.13; N 56.72; H 2.71. IR (cm^{-1}, KBr pellets): 3415, 3368m (νNH_2), 3225, 3188m (νN–H), 1658s (νC=N, N=N), 1563w (δC–N, N–N), 1469w (δNH), 1384vs, 1308m (νNO_3^-), 1079, 732, 445w (δ ring bone) [8].

2.2. Physical techniques

C, H, N were determined using a Flash EA 1112 fully automatic microanalyzer. Infrared spectra were recorded on a Bruker Equinox 55 infrared spectrometer as KBr microdiscs in the wavenumber range 4000–400 cm^{-1} with a resolution of 4 cm^{-1}. DSC and TG measurements were carried out using Perkin Elmer Pyris-1 differential scanning calorimeter and thermogravimetric balance, respectively, using dry nitrogen as atmosphere with a pressure of 0.2 MPa. The crystal samples were sealed in aluminum pans for DSC experiments and were heated from 50 to 600 °C at heating rates of 2, 5, 10, 15, 20 and 25 °C/min. In TG experiments, the crystal samples were held in platinum pans and were heated from 50 to 600 °C at a heating rate of 10 °C/min.

2.3. X-ray data collection and structure refinement

A suitable crystal (0.50 mm × 0.30 mm × 0.20 mm) was mounted on a glass fiber, coated with epoxy and placed on the goniometer of a Siemens P4 fully automatic four-circle diffractometer. Unit cell parameters were determined by least-squares analysis of 30 reflections with $6.8^\circ < \theta < 14.73^\circ$ using ω-scans at 296 ± 2 K with graphite monochromatized Mo Kα radiation ($\lambda = 7.1073$ nm). 1286 reflections were collected between $1.92^\circ < \theta < 25.23^\circ$ yielding 984 unique reflections ($R_{int} = 0.0351$). Information concerning crystallographic data collection and structure refinement is summarized in Table 1. No absorption correction was applied to the intensity data.

The structure was solved by the direct methods routine of SHELXS-97 [10] in the space group $P2_1/c$, and subsequent difference-Fourier map revealed the positions of the remaining atoms. All non-hydrogen atoms were refined anisotropically using a full-matrix least-squares procedure on F^2 with SHELXL-97 [11], and all hydrogen atoms were treated isotropically. The atomic coordinates and displacement parameters, selected bond distances and angles are listed in Tables 2–4.

Table 1
Crystal data and structure refinement parameters for 5-ATZN

Empirical formula	$CH_4N_6O_3$
Molar mass (g/mol)	148.1
Crystal system	Monoclinic
Space group	$P2_1/c$
a (nm)	1.0606(2)
b (nm)	0.35065(4)
c (nm)	1.4641(2)
β (°)	90.63(1)
V (nm^3)	0.54(1)
Z	4
D_c (g/cm^3)	1.807
μ(Mo Kα) (mm^{-1})	0.168
F(0 0 0)	304
Crystal size (mm)	0.50 × 0.30 × 0.20
θ range (°)	1.92–25.23
Measured reflections	1286
Independent reflections [$R_{int} = 0.0180$]	984
R_1, wR_2 [$I > 2\sigma(I)$]	0.0364, 0.0958
R_1, wR_2 (all data)	0.0448, 0.0990
δp_{max}, δp_{min} (e/nm^3)	163, −200

3. Results and discussion

3.1. Thermal decomposition mechanism

The DSC and TG-DTG curves are shown in Figs. 1 and 2, respectively. Infrared spectra were used to distinguish the solid residues at different temperatures (Fig. 3).

Under the linear heating rate of 10 °C/min with nitrogen atmosphere, 5-ATZN is stable until 193 °C/min when an intense exothermic decomposition process (246 J/g) begins, and ends at 202 °C. The peak temperature is 198 °C. The melting of 5-ATZN, which had been reported by Burns and Khandhadia [3,4], was not observed in this study. This may be attributed to the higher purity of the crystal samples, the different method of synthesis and the different experimental conditions. Corresponding to this exotherm, there is a mass loss of 18.0% of the initial mass on the TG curve in the temperature range 171–202 °C, and the maximum rate of mass loss of 7.1%/min was observed at 191 °C.

Table 2
Non-hydrogen atomic coordinates (×10^4) and equivalent isotropic displacement parameters ($10^5 \times nm^3$) for 5-ATZN

Atom	x	y	z	U (eq)
O(1)	3825(1)	6983(5)	1985(1)	47(1)
O(2)	2276(1)	4276(5)	1262(1)	39(1)
O(3)	3819(1)	6702(5)	511(1)	49(1)
N(1)	1563(2)	2178(5)	4469(1)	33(1)
N(2)	335(2)	2464(6)	4184(1)	38(1)
N(3)	325(2)	3246(6)	3342(1)	39(1)
N(4)	1548(2)	3510(5)	3059(1)	33(1)
N(5)	3558(2)	2809(6)	3763(1)	42(1)
N(6)	3328(1)	6018(6)	1253(1)	34(1)
C	2326(2)	2832(6)	3764(1)	29(1)

U (eq) is defined as one-third of the trace of the orthogonalized U^{ij} tensor.

Table 3
Selected bond distances (nm) and angles (°)

Bond	Distance
N(2)–N(3)	0.1262(2)
N(3)–N(4)	0.1368(2)
N(4)–C	0.1335(2)
N(1)–H(1)	0.102(2)
N(5)–H(5A)	0.084(2)
O(1)–N(6)	0.12369(19)
O(3)–N(6)	0.12339(19)
N(1)–C	0.1338(2)
N(5)–C	0.1307(2)
N(1)–N(2)	0.1367(2)
N(4)–H(4)	0.103(2)
N(5)–H(5B)	0.087(2)
O(2)–N(6)	0.1272(2)
Bond	**Angle**
C–N(1)–N(2)	109.53(15)
N(3)–N(2)–N(1)	108.17(16)
N(4)–C–N(1)	104.61(16)
N(5)–C–N(4)	127.56(17)
N(2)–N(3)–N(4)	108.18(15)
C–N(4)–N(3)	109.51(14)
N(5)–C–N(1)	127.82(17)

The IR spectrum of the solid residue at 210 °C is similar to that of 5-ATZ [8], so the decomposition reaction is suggested to be

$$\text{5-ATZN} \rightarrow \text{5-ATZ} + HNO_3 \quad (1)$$

$$HNO_3 \rightarrow H_2O + NO_2 \quad (2)$$

H_2O (g) and NO_2 are the gas products of the thermal decomposition of 5-ATZN in this process. The very weak bands at 1388 and 1323 cm^{-1} indicate that some of NO_3^- is still retained in the condensed phase after the decomposition. So the mass loss on the TG curve is lower than expected by Eq. (1) (42.55%). Such a decomposition route is different from the conclusion made by Brill and Ramanathan [8], who pointed out that the direct decomposition of $[5\text{-ATZH}]^+$ is favored by the longer reaction time in the lower temperature range.

The second exothermic decomposition (508 J/g) occurs intensely between 224 and 238 and the peak temperature is 234 °C. This process is accompanied by a mass loss of 26.8% in the temperature range 210–270 °C (the calculated value by Eq. (3) is 29.05%), and the maximum rate of mass loss is at 224 °C. In the IR spectrum of the solid residue at 280 °C, the characteristic bands of NO_3^- disappear and the band at 1571 cm^{-1} is strengthened. The spectrum resembles that of melamine [5,6]. The decomposition process can be described as

$$\text{5-ATZ} \rightarrow HN_3 + NH_2CN \quad (3)$$

$$3NH_2CN \rightarrow \text{melamine} \quad (4)$$

In order to capture the N_3^- in the gas phase, 5-ATZN was mixed with KOH, and heated to 280 °C. The characteristic

Table 4
Hydrogen bond distances (nm) and angles (°)

D	H	A	D–H distance	H...A distance	D...A distance	D–H...A angle
N1	H1	O2	0.102(2)	0.176(2)	0.27716(19)	177(2)
N4	H4	O2	0.103(2)	0.174(2)	0.27639(19)	172(3)
N5	H5A	O1	0.084(2)	0.229(2)	0.3002(2)	144(2)
N5	H5B	O3	0.087(2)	0.229(2)	0.3018(2)	141(2)

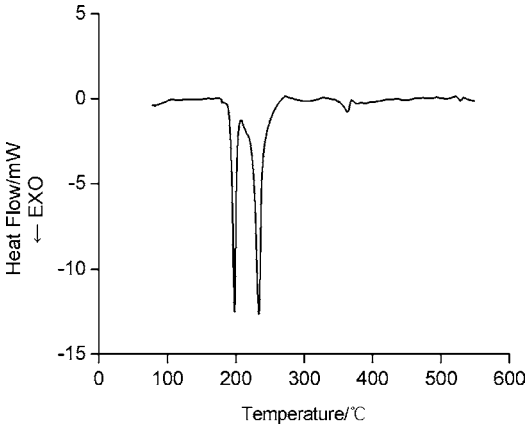

Fig. 1. The DSC curve of 5-ATZN under N_2 atmosphere with a heating rate of 10 °C/min.

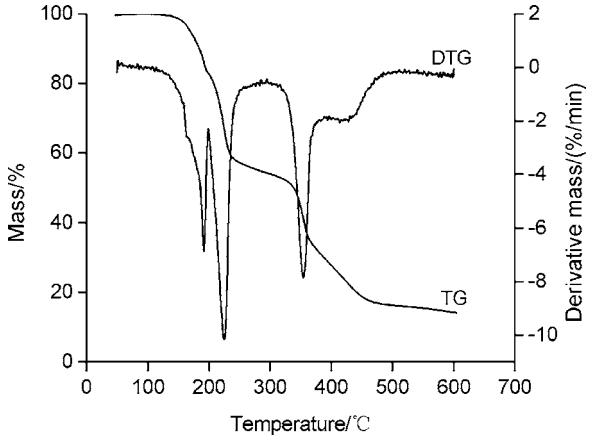

Fig. 2. The TG–DTG curves of 5-ATZN under N_2 atmosphere with a heating rate of 10 °C/min.

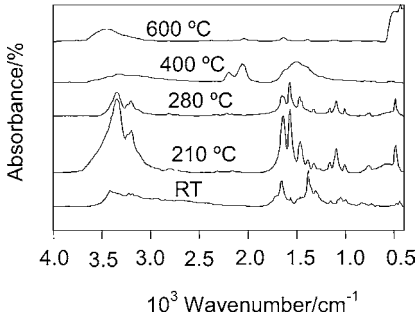

Fig. 3. The FT-IR spectra of the solid residues at different temperatures.

bands at 2175 and 2053 cm^{-1} in the spectrum of the solid residue are identified as N_3^-. This proves the formation of HN_3 gas as a product of the thermal decomposition of 5-ATZN.

The further exothermic decomposition begins at 354 °C and ends at 368 °C with a lower enthalpy change of 21 J/g, and the peak temperature is 363 °C. Corresponding to this exothermic decomposition there is a mass loss of 28.1% on the TG curve between 335 and 401 °C. The solid residue at 400 °C is identified as melem by the characteristic bands at 2198, 2055 cm^{-1} and NH_3 is assumed to be the gaseous product [7].

$$\text{melamine} \xrightarrow{2NH_3} \text{melem} \quad (5)$$

On the TG curve, there still is a slow mass loss of 12.2% from 402 to 600 °C with no detectable peaks on the DSC curve. The mass of the final residue is 14.3% of the initial mass, and the residue is identified as melon-like product by IR bands at 2042, 1635, 1122 cm^{-1} [6].

$$\text{melem} \xrightarrow[-NH_3]{} \text{melon} \quad (6)$$

The formation of thermally stable solid residues, such as cyclic azines, melamine, melem and melon, might decrease the heat and mass transfer at the burning surface, so 5-ATZN should be an effective additive in composite gas propellants.

3.2. Non-isothermal kinetics analysis

Identification of chemical kinetics parameters is a prominent field of basic research in energetic materials and composite gas propellants. Kissinger's method [12] and Ozawa–Doyle's method [13,14] are widely used to determine the apparent activation energy (E) and the pre-exponential factor (A). In these two methods, the thermal decomposition is assumed not to be a complex reaction. In Kissinger's method, the reaction function is assumed as

$$f(\alpha) = (1-\alpha)^n \quad (7)$$

Table 5
The peak temperatures of the first exotherm at different heating rates and the chemical kinetics parameters

Heating rates (°C/min)	Peak temperatures (°C)
2	191.1 ± 0.2
5	193.6 ± 0.3
10	198.5 ± 0.3
15	200.1 ± 0.5
20	203.0 ± 0.4
25	205.2 ± 0.3
Calculation results by Kissinger's method	
E (kJ/mol)	311.0 ± 5.8
$\ln A$ (s^{-1})	75.8 ± 1.4
Calculation results by Ozawa–Doyle's method	
E (kJ/mol)	303.2 ± 5.6

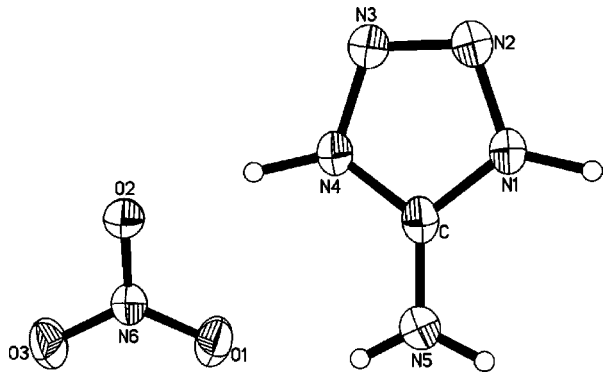

Fig. 4. The molecular structure and atomic numbering scheme of 5-ATZN.

The plot of $\ln(\varphi/T^2)$ versus T^{-1} is linear (φ is the heating rate). The values of the slope and the intercept are related with the parameters E and A, respectively. Ozawa–Doyle's method is unrelated to the mechanism function, and the plot of $\ln\varphi$ versus T^{-1} is linear. The slope is also used to determine the value of E.

Although the thermal decomposition of 5-ATZN is complex, Kissinger's method and Ozawa–Doyle's method were used to estimate the kinetic parameters, based on the first exothermic peak temperatures measured at six different heating rates of 2, 5, 10, 15, 20 and 25 °C/min. The peak temperatures and the calculation results are listed in Table 5.

3.3. Molecular structure

The molecular structure of 5-ATZN was determined by X-ray single-crystal diffraction. A single unit cell with the atomic numbering scheme and atom connectivity is shown in Fig. 4. 5-ATZN is identified as an ionic salt, and consists of $[5\text{-ATZH}]^+$ cations and NO_3^- anions, which are linked together through electrostatic interactions and extensive hydrogen bonds (Fig. 5).

Owing to the protonation of the 4-N, the connective character of the $[5\text{-ATZH}]^+$ ring is different from that of 5-ATZ. The N2–N3, C–N1 and C–N4 bond distances are shorter, while the N1–N2 and N3–N4 distances are longer compared with 5-ATZ [8]. The longer N1–N2 and N3–N4 bonds favor the loss of N_2 from $[5\text{-ATZH}]^+$, while the loss of HN_3 from 5-ATZ is favored by the longer C–N bond. The similar bond distances of CN1 and CN4 in $[5\text{-ATZH}]^+$ indicate that there is delocalization in N4–C–N1, which strengthens the stable structure. The bond distances of

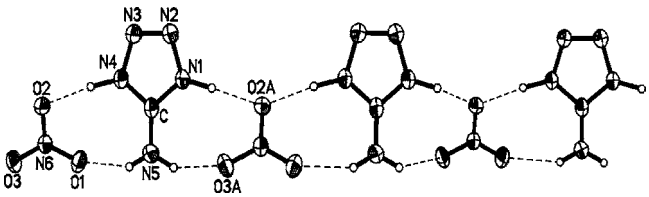

Fig. 5. The hydrogen bonds in 5-ATZN.

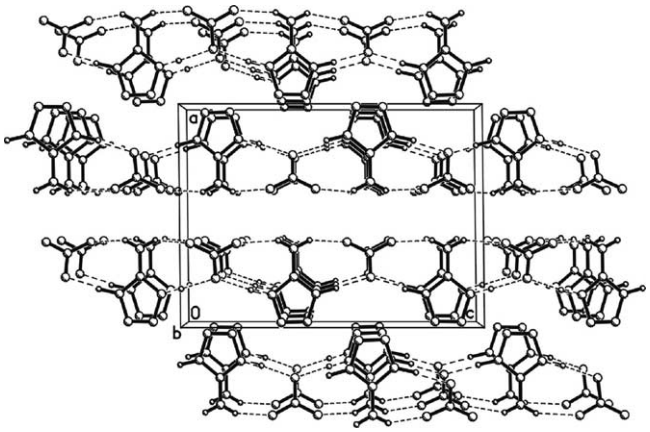

Fig. 6. The packing arrangement of 5-ATZN.

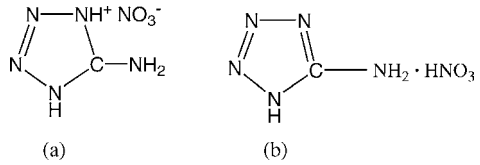

Fig. 7. Two structural formulas of 5-ATZN: (a) obtained structural formula and (b) presumed structural formula.

$[5\text{-ATZH}]^+$ resolved by X-ray single-crystal diffraction are consistent with the results of semi-empirical molecular orbital calculations made by Brill and Ramanathan [8]. The N2–N3 bond distances in both results are 0.1262 nm, and the N1–N2 and N3–N4 bond distances are 0.1367(2) and 0.1368(2) nm in our study, and are 0.1358 nm in Brill's result. The C–N bond (0.1338(2) nm) is apparently shorter than the semi-empirical result (0.1411 nm), which then leads to a smaller sum of the bond distances (0.667 nm) compared with the result obtained by Brill (0.680 nm). So $[5\text{-ATZH}]^+$ is expected to be more stable.

The $[5\text{-ATZH}]^+$ cations and NO_3^- anions are linked into 2D layered structures by electrostatic interaction and hydrogen bonds (see Fig. 6). The N1 and N4 atoms act as donors in the hydrogen bonds with O2 as acceptors, and the angles of this kind of hydrogen bonds are nearly 180°. The N5 atom acts as donor in hydrogen bonds with O1 and O3 as acceptors. These extensive intermolecular hydrogen bonds make an important contribution to the stability of the title compound.

Our molecular structure determination proved that 5-ATZN is a kind of ionic salt, and that the 4-N is involved in the salt formation (see Fig. 7(a)). It is different from the earlier presumption, which presumed that the amino group was involved in the salt formation [15]. In US patents 3,734,789 and 3,898,112 [1,2], 5-ATZN was depicted by the structural formula as shown in Fig. 7(b).

4. Conclusion

The thermal decomposition of 5-ATZN occurs via the 5-ATZ decomposition route and forms a measurable amount of thermally stable melon-like solid residue. The thermal stable cyclic azines are expected to modify combustion of composite gas propellants. This study was done at low heating rates and low pressures, so conditions would be very different from those under combustion conditions. Nevertheless, the thermally stable azines would still be expected to form and to modify propellant combustion.

References

[1] A.H.S. Ruediger, S.H. Hermann, US Patent 3,898,112 (1975).
[2] K.M. Bertram, J.P. Frank, US Patent 3,734,789 (1973).
[3] S.P. Burns, P.S. Khandhadia, US Patent 6,287,400 (2001).
[4] S.P. Burns, P.S. Khandhadia, US Patent 6,475,312 (2002).
[5] C.E. Stoner Jr., T.B. Brill, Combust. Flame 83 (1991) 302–308.
[6] A. Gao, Y. Oyumi, T.B. Brill, Combust. Flame 83 (1991) 345–352.
[7] G.K. Williams, S.F. Palopoli, T.B. Brill, Combust. Flame 98 (1994) 197–204.
[8] T.B. Brill, H. Ramanathan, Combust. Flame 122 (2000) 165–171.
[9] J.G. Zhang, T.L. Zhang, K.B. Yu, Initiators Pyrotech. 3 (1999) 1–4 (in Chinese).
[10] G.M. Sheldrick, SHELXS-97, Acta. Crystallogr. Sect. A 46 (1990) 467.
[11] G.M. Sheldrick, SHELXL-97, Program for crystal structure refinement from diffraction data, University of Göttingen, Göttingen, Germany, 1997.
[12] H.E. Kissinger, Anal. Chem. 29 (11) (1957) 1702–1706.
[13] T. Ozawa, Bull. Chem. Soc. Jpn. 38 (11) (1965) 1881–1885.
[14] C.D. Doyle, J. Appl. Polym. Sci. 5 (1961) 285–287.
[15] R.M. Herbst, J.A. Garrison, J. Org. Chem. 18 (8) (1953) 941–945.